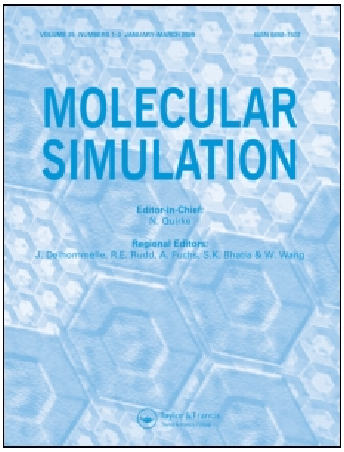

Molecular Simulation
Publication details, including instructions for authors and subscription information:
http://www.informaworld.com/smpp/title~content=t713644482

Effects of the side pockets on gas separation in metal-organic framework Cu-BTC: a molecular simulation study

Chunyu Xue[a]; Qingyuan Yang[a]; Chongli Zhong[a]
[a] Lab of Computational Chemistry, Department of Chemical Engineering, Beijing University of Chemical Technology, Beijing, People's Republic of China

To cite this Article Xue, Chunyu , Yang, Qingyuan and Zhong, Chongli(2009) 'Effects of the side pockets on gas separation in metal-organic framework Cu-BTC: a molecular simulation study', Molecular Simulation, 35: 15, 1249 — 1255

To link to this Article: DOI: 10.1080/08927020902988865

URL: http://dx.doi.org/10.1080/08927020902988865

Molecular Simulation
Vol. 35, No. 15, December 2009, 1249–1255

Effects of the side pockets on gas separation in metal-organic framework Cu-BTC: a molecular simulation study

Chunyu Xue, Qingyuan Yang and Chongli Zhong*

Lab of Computational Chemistry, Department of Chemical Engineering, Beijing University of Chemical Technology, Beijing 100029, People's Republic of China

(*Received 19 February 2009; final version received 18 April 2009*)

The effects of the side pockets on gas separation in Cu-BTC were studied by performing molecular simulations on six binary mixtures in Cu-BTC with and without blocking the side pockets. The results show that the side pockets not only affect the selectivity behaviour greatly, but also enhance the selectivity significantly, particularly at pressures lower than 1.0 MPa. In addition, this work shows that the contribution of the side pockets can be related to the interactions between the adsorbate and Cu-BTC: the larger the difference in interactions of the adsorbates with Cu-BTC, the bigger the contribution of the pockets. Furthermore, this work shows that, at moderate pressures, the presence of side pockets can enhance selectivity by 30–50%, illustrating that for practical applications the presence of side pockets is beneficial for gas separation.

Keywords: pocket effect; separation; metal-organic frameworks; simulation

1. Introduction

Metal-organic frameworks (MOF) are a new family of nanoporous materials with various promising applications, which are attributed to their flexibility to design through controlling of the architecture and chemical functionality of the pores [1–3]. Among the various MOF synthesised, Cu-BTC with a channel/pocket complex framework is a typical representative that has attracted great attention since it was first reported by Chui et al. [4]. To date, great efforts have been made to improve the synthesis and activation of Cu-BTC experimentally [5–11], which mainly focus on gas-adsorption properties, particularly on hydrogen storage. On the other hand, theoretical investigations have also been carried out on the adsorption [12,13], separation [14–16] and diffusion [17,18] in this material.

One of the main characteristics of Cu-BTC is that it has octahedron-shaped side pockets, which play an important role in the adsorption separation of mixtures [15,16,19]. For example, Krungleviciute et al. [19] found that the smaller octahedron-shaped side pockets in this material are accessible to Ar but not to CF_4 experimentally and thus can be beneficial for separation of CF_4/Ar mixtures. Our previous simulations [15] on the $CO_2/CH_4/H_2$ separations in Cu-BTC showed that the side pockets play the dominant role in determining the selectivity behaviours in Cu-BTC at the lower pressure ranges. Therefore, it is important to understand how and to what extent the side pockets influence gas separation; however, such a systematic study is not available in MOF to date. This information is very difficult to obtain by experimental methods, while molecular simulation is a powerful tool to give deep insights into the question at the molecular level. Thus, in this work a systematic molecular simulation study was performed to understand the effect of side pockets on gas separation in Cu-BTC.

2. Model and computational details

2.1 MOF structure

The crystal structure of Cu-BTC was constructed from the XRD data [4] using a Materials Visualizer, [20] and the unit cell is shown in Figure 1(a). Cu-BTC has a 3D channel structure of *ca.* 0.9 nm diameter connecting a system of octahedron-shaped cages of *ca.* 0.5 nm (Figure 1(b)) accessible through small windows (3.5 Å in diameter). It should be pointed out that the crystal structure of Cu-BTC includes axial oxygen atoms weakly bonded to the Cu atoms, which correspond to the water ligands. Our simulations were performed on dry Cu-BTC with these oxygen atoms removed (activated Cu-BTC that is used in adsorption experiments), and thus the diameter of the triangular windows is *ca.* 4.6 Å, which are wide enough to allow the studied adsorbate molecules to enter the pockets.

2.2 Force field

The force field plays an important role in molecular simulations. In this work, a single Lennard-Jones (LJ) interaction site model was used to describe both CH_4 [21] and Ar [22] molecules. CO_2 was modelled as a rigid linear

---

*Corresponding author. Email: zhongcl@mail.buct.edu.cn

ISSN 0892-7022 print/ISSN 1029-0435 online

DOI: 10.1080/08927020902988865
http://www.informaworld.com

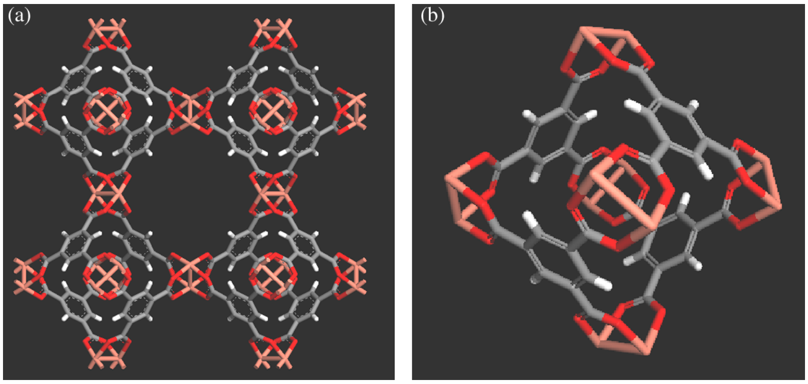

Figure 1. (a) The unit cell crystal structure of Cu-BTC, (b) the structure of one octahedron-shaped side pocket (Cu, pink; O, red; C, grey; hydrogen, white).

triatomic molecule, and each atom was represented as a LJ-interaction site with charges located on each site to represent its quadrupole moment [23]. N_2 was represented as a three-site model with two sites located at two atoms of one molecule and the third one located at its centre of mass (COM) [23]. The partial point charges located at each LJ site can represent its quadrupole moment. As for H_2, it was treated as a diatomic molecule modelled by an LJ core located at its COM and three partial charges with two located at the H atoms and one at the centre between the two H atoms [24]. The above potential models have been successfully used to model the adsorption of CH_4 [25–27], CO_2 [14,15,28], N_2 [14,29] and H_2 [30–32] in MOF and other porous materials. For the atoms in the framework of Cu-BTC, the universal force field of Rappe et al. [33] was adopted, which has also been successfully used to depict the adsorption [30,34], diffusion [17,18,35], and separation [36–38] of several light gases and their mixtures in MOF. The potential parameters used in this work are listed in Table 1. All the LJ cross-interaction parameters were determined by the Lorentz–Berthelot mixing rules.

A recent review by Liu et al. [11] for H_2 adsorption in Cu-BTC shows that the preparation and activation process has a significant impact on the adsorption capacity, surface area and pore volume. Their carefully prepared Cu-BTC samples exhibit the largest pore volume and H_2 adsorption amount to date. Thus, their data were adopted to further confirm the reliability of the above set of force fields adopted in this work, and the simulated adsorption isotherms for Ar, N_2 and H_2 in Cu-BTC at 298 K are shown in Figure 2(a) and (b), where the corresponding experimental data [11] are also included for comparison. Obviously, the results show that the simulation results give a good agreement with the experimental adsorption isotherms, further validating the reliability of the force fields adopted. The adsorption isotherms for CO_2 and CH_4 were also calculated, and compared with the experimental data [5,39], as shown in Figure 2(c) and (d). Obviously, the simulated results overestimated the experimental data, particularly for CO_2 at higher pressure. This may be attributed to the samples obtained having a much lower pore volume compared with those of the ideal crystal

Table 1. The LJ potential parameters for the adsorbates and Cu-BTC used in this work.

	Ref		σ (Å)	ε/k_b (K)	q (e)
CH_4	[21]	CH_4	3.73	148.0	0.00
Ar	[22]	Ar	3.40	119.8	0.00
CO_2 (C—O distance: 1.16 Å)	[23]	C	2.80	27.0	0.70
		O	3.05	79.0	−0.35
N_2 (N—N distance: 1.10 Å)	[23]	N	3.31	36.0	−0.482
		COM	0.00	0.00	0.964
H_2 (H—H distance: 0.74 Å)	[24]	H	0.00	0.00	0.468
		COM	2.958	36.7	−0.936
Cu-BTC	[15,33]	O	3.12	30.19	−0.665
		C1[a]	3.43	52.84	0.778
		C2[a]	3.43	52.84	−0.092
		C3[a]	3.43	52.84	−0.014
		H	2.57	22.14	0.109
		Cu	3.11	2.52	1.098

[a] The atom types were defined in our previous work [15].

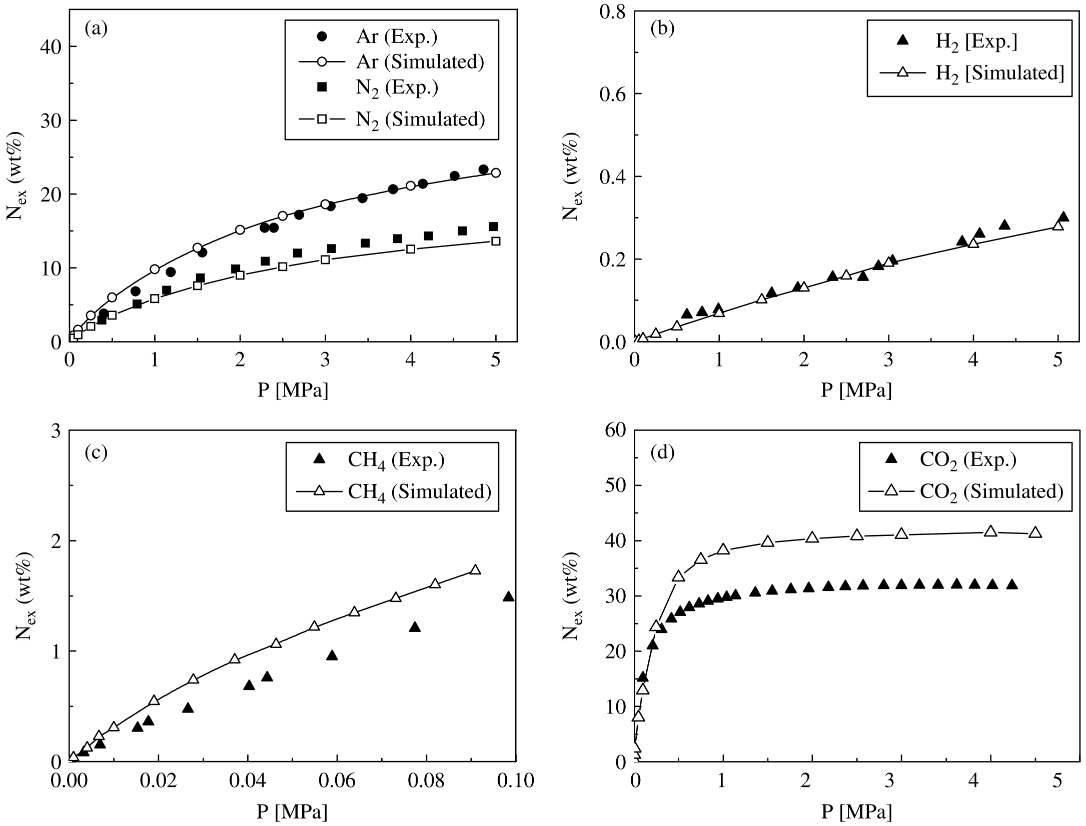

Figure 2. Experimental [5,11,39] and simulated adsorption isotherms of pure gases in Cu-BTC: (a) Ar and N_2 at 298 K, (b) H_2 at 298 K, (c) CH_4 at 295 K (d) CO_2 at 298 K.

as well as the Cu-BTC samples carefully prepared by Liu et al. [11], thus, the amount of CO_2 and CH_4 adsorbed in Cu-BTC by Wang et al. [5] and Millward et al. [39] could be experimentally underestimated. However, it is thought that these disagreements between the simulated results and the experimental data would not affect the qualitative discussions about the blocking effects of the side pockets on the selectivity behaviours in Cu-BTC.

2.3 Simulation details

The Grand Canonical Monte Carlo (GCMC) simulations were employed to calculate the adsorption of pure gases and their mixtures in Cu-BTC. The number of the unit cells adopted in the simulation box varied from $2 \times 2 \times 2$ to $4 \times 4 \times 4$ so that enough molecules were accommodated to guarantee the simulation accuracy. The framework of Cu-BTC kept rigid during the simulations. A cutoff radius of 15.0 Å was applied to all the LJ interactions, and the electrostatic interactions in all simulations were handled by the Ewald summation technique. The partial point charges of all the framework atoms in Cu-BTC were taken from our previous work [15], as shown in Table 1, which were calculated by the DFT method. The periodic boundary conditions were applied in all the three dimensions. For each state point, GCMC simulation consisted of 1.0×10^7 steps to guarantee the equilibration, followed by 1.0×10^7 steps to sample the desired thermodynamic properties. As all the atoms in the adsorbent were assumed to be fixed in their crystallographic positions, the potential energies between an adsorbate and the adsorbent were initially tabulated on a series of three-dimensional grid points with a grid spacing of 0.15 Å. During the simulations, the potential energy at any position in the adsorbent was determined by interpolation. The bulk fugacity required in the GCMC simulations was calculated by Peng–Robinson equation of state. Details on the method can be found elsewhere [40].

3. Results and discussion

3.1 Adsorption selectivity behaviours in Cu-BTC with and without blocking the side pockets

In the separation processes a good indication of the ability for separation is the selectivity of a porous material for different components in the mixtures. The selectivity for component *A* relative to component *B* is defined by $S = (x_A/x_B)(y_B/y_A)$, where x_A and x_B are the mole fractions of components *A* and *B* in the adsorbed phase, while y_A and

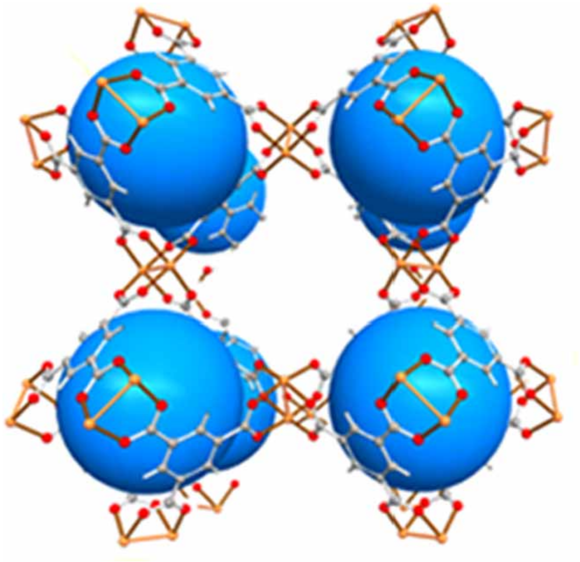

Figure 3. The crystal structure of Cu-BTC with the side pockets blocked.

y_B are the mole fractions of components *A* and *B* in the bulk phase, respectively.

As the first step to study the effects of side pockets on separation, adsorption selectivities were calculated by the GCMC simulations at 298 K for six binary mixtures (CH_4/H_2, CH_4/N_2, N_2/H_2, CO_2/N_2, CO_2/H_2, and CO_2/CH_4) in Cu-BTC with and without blocking the side pockets. These six systems selected in this work have practical applications with different features, and the blocked Cu-BTC was obtained by putting hard balls into the side pockets to make the pockets inaccessible to the adsorbates as indicated in Figure 3. Figure 4 shows the simulated results for the adsorption selectivities of these six systems in non-blocked and blocked Cu-BTC at 298 K, as a function of the pressure up to 5.0 MPa. As can be seen from this figure, for each mixture examined in this work, the blocked Cu-BTC shows a very different separation behaviour compared with that in the non-blocked case, particularly at pressures lower than 1.0 MPa, and the difference is greatly dependent on the nature of the system for separation.

Our previous works have showed that, for Cu-BTC, the side pockets with the smaller pore sizes have the stronger electrostatic field as well as the confinement effects compared with the channel pores, which results in the side pockets being the preferential adsorption sites for the adsorbate molecules [12,15]. The results shown in Figure 4 evidently indicate that the blocking of the side pockets could cause the remarkable differences in the selectivity curves at the lower-pressure regions. Furthermore, this phenomenon occurs at a different pressure range for various systems and this may be attributed to the different saturation adsorption pressure in the side pocket for a certain mixture, which depends on the nature of the examined mixtures.

For the mixture of CH_4/H_2, the difference between the selectivity curves in the blocked and non-blocked cases is that a sharp decrease in the latter occurred at the lower-pressure regions. This is caused by the competition between the entropic and energetic contributions in those side pockets, i.e. the entropic effects favour the adsorption of the smaller H_2 molecules while the energetic contributions favour the larger CH_4 molecules, which is inclined to the adsorption of the former with the increase of pressure. This reason also holds true in the cases of the CH_4/N_2 and N_2/H_2 mixtures. For the mixtures involving CO_2, a quick decrease or increase was observed in the non-blocked structure in comparison with the curve in the blocked one at a low pressure. It can be explained as follows: due to the packing effects of adsorbate molecules decreasing in the following order: $H_2 > N_2 > CH_4$, and the strong electrostatic contributions favouring the adsorption of CO_2 with a larger quadrupole moment, the first trend was changed from a quick decrease in Figure 4(d) to increasing in Figure 4(f) for those mixtures in the Cu-BTC. Furthermore, the selectivity behaviours shown in Figure 4 illustrate that the side pockets can influence the selectivity performance largely up to moderate pressure, thus they are important in practical applications.

3.2 Effects of side pockets on adsorption selectivity in Cu-BTC

The selectivity in the non-blocked Cu-BTC is larger than that in the blocked for all the systems as shown in Figure 4, indicating that the side pocket can enhance adsorption selectivity. To have a better understanding of the effects of the side pockets on adsorption selectivity, the relative selectivity, defined as $S_r = S/S_b$, where S and S_b denote the selectivity in the non-blocked and blocked Cu-BTC, respectively, were further calculated at 298 K, as shown in Figure 5, as a function of pressure. Figure 5 shows that the enhancement of separation selectivity by the presence of side pockets generally decreases with the pressure increasing; the only exception is the CO_2/CH_4 system. At a low-pressure region, the selectivity can be enhanced approximately by 2–3 times, while at moderate pressures for a practical application, the enhancement is also evident (*ca.* 30–50%); this demonstrates that the presence of side pockets is beneficial for separation in practical applications.

To further understand for which system the effect of side pockets is more evident, the ratio of isosteric heat of adsorption at an infinite dilution for component *A* relative to component *B*, $Q_r = Q_A/Q_B$, was calculated, where Q_A and Q_B are the isosteric heat of adsorption at an infinite dilution of the components *A* and *B* in Cu-BTC at 298 K, respectively. The relationships between the relative selectivity S_r at infinite dilute and Q_r are shown in Figure 6. Obviously,

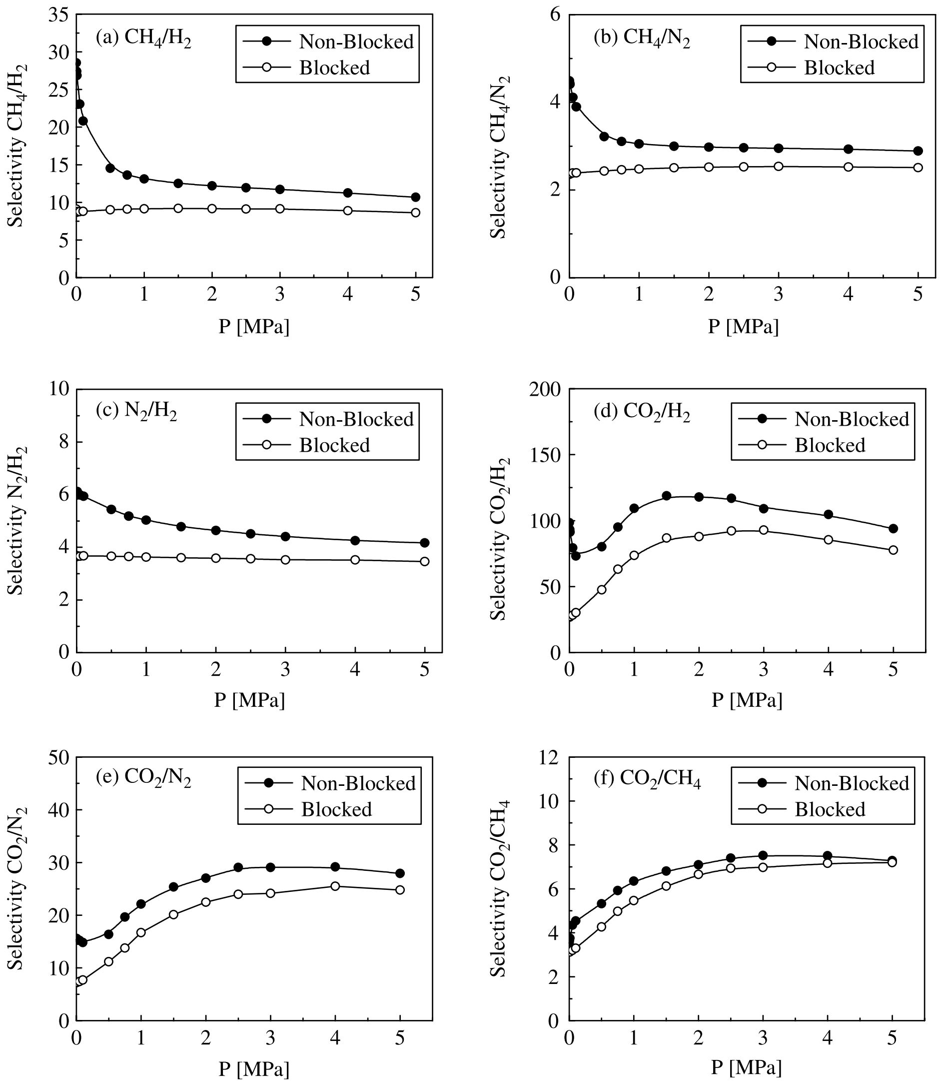

Figure 4. The selectivity for six binary equimolar mixtures in both the non-blocked and blocked Cu-BTC at 298 K.

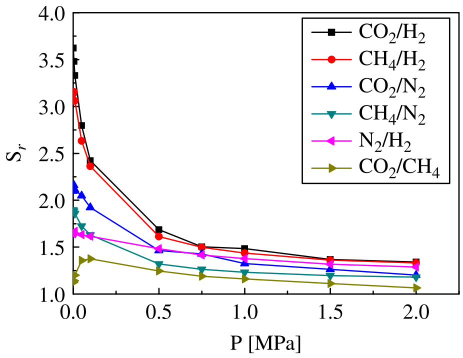

Figure 5. The relative selectivities of binary equimolar mixtures in Cu-BTC at 298 K.

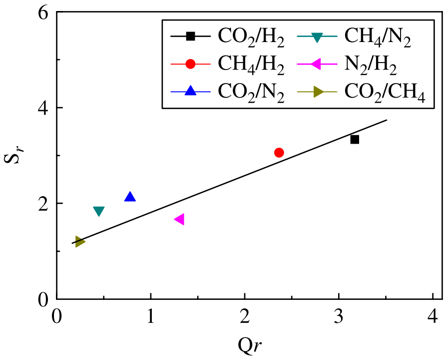

Figure 6. The relative selectivity at 1 MPa versus isosteric heat-of-adsorption ratio at 298 K.

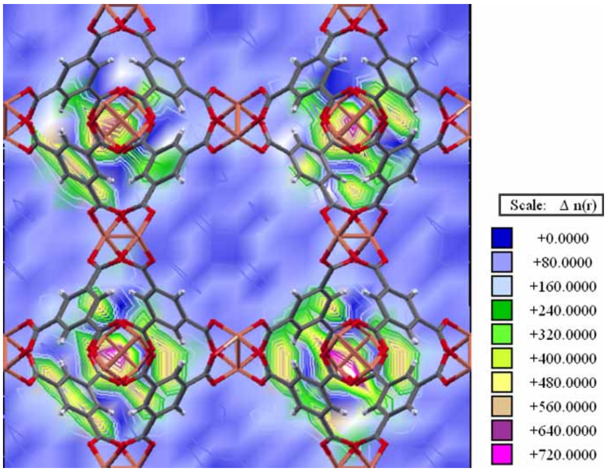

Figure 7. The selectivity distribution of CO_2/H_2 in Cu-BTC at 1 MPa and 298 K.

the larger the Q_r, the bigger the S_r. It is also found at moderate pressures. Therefore, we may conclude that the side pockets are more beneficial for systems with a larger difference in the energetic interactions of adsorbates with Cu-BTC.

Finally, the selectivity distribution of an equimolar mixture of CO_2/H_2 in Cu-BTC at 1 MPa and 298 K was calculated and shown in Figure 7 as an example to give a direct visualisation of the role of the side pockets. Obviously, the selectivity in the side pocket is much larger than that in the other regions, directly showing the positive contribution of the side pockets to separation.

4. Conclusion

This work shows that both the selectivity behaviour and the values are affected largely by the presence of side pockets in Cu-BTC. The effect is more evident at the lower pressures, which can increase the selectivity by 2–3 times at very low pressures, and 30–50% at moderate pressures. Moreover, this work shows that the contribution of the side pockets can be related to the interactions between the adsorbate and Cu-BTC: the larger the difference in the interactions of the adsorbates with Cu-BTC, the bigger the contribution of the pockets. The information obtained clarifies the effects of the side pockets in Cu-BTC, and also shows that for practical applications, the presence of side pockets is beneficial for gas separation.

Acknowledgements

The financial support of the National Natural Science Foundation of China (Nos 20725622, 20876006, 20821004, 20706002) is greatly appreciated.

References

[1] G. Férey, *Hybrid porous solids: past, present, future*, Chem. Soc. Rev. 37 (2008), pp. 191–214.

[2] R.E. Morris and P.S. Wheatley, *Gas storage in nanoporous materials*, Angew. Chem. Int. Ed. 47 (2008), pp. 4966–4981.

[3] S. Horike, M. Dinca, K. Tamaki, and J.R. Long, *Size-selective lewis acid catalysis in a microporous metal-organic framework with exposed* Mn^{2+} *coordination sites*, J. Am. Chem. Soc. 130 (2008), pp. 5854–5855.

[4] S.S. Chui, S.M. Lo, J.P. Charmant, A.G. Orpen, and I.D. Williams, *A chemically functionalizable nanoporous material* $[Cu_3(TMA)_2(H_2O)_3]n$, Science 283 (1999), pp. 1148–1150.

[5] Q.M. Wang, D.M. Shen, M. Bulow, M.L. Lau, S.G. Deng, F.R. Fitch, N.O. Lemcoff, and J. Semanscin, *Metallo-organic molecular sieve for gas separation and purification*, Microporous Mesoporous Mater. 55 (2002), pp. 217–230.

[6] K. Schlichte, T. Kratzke, and S. Kaskel, *Improved synthesis, thermal stability and catalytic properties of the metal-organic framework compound* $Cu_3(BTC)_2$, Microporous Mesoporous Mater. 73 (2004), pp. 81–88.

[7] U. Mueller, M. Schubert, F. Teich, H. Puetter, K. Schierle-Arndt, and J. Pastre, *Metal-organic frameworks-Prospective industrial applications*, J. Mater. Chem. 16 (2006), pp. 626–636.

[8] P. Krawiec, M. Kramer, M. Sabo, R. Kunschke, H. Frode, and S. Kaskel, *Improved hydrogen storage in the metal-organic framework* $Cu_3(BTC)_2$, Adv. Eng. Mater. 8 (2006), pp. 293–296.

[9] J.L.C. Rowsell and O.M. Yaghi, *Effects of functionalization, catenation, and variation of the metal oxide and organic linking units on the low-pressure hydrogen adsorption properties of metal-organic frameworks*, J. Am. Chem. Soc. 128 (2006), pp. 1304–1305.

[10] B. Xiao, P.S. Wheatley, X.B. Zhao, A.J. Fletcher, S. Fox, A.G. Rossi, S. Megson, S. Bordiga, L. Regli, K.M. Thomas, and R.E. Morris, *High-capacity hydrogen and nitric oxide adsorption and storage in a metal-organic framework*, J. Am. Chem. Soc. 129 (2007), pp. 1203–1209.

[11] J.C. Liu, J.T. Culp, S. Natesakhawat, B.C. Bockrath, B. Zande, S.G. Sankar, G. Garberoglio, and J.K. Johnson, *Experimental and theoretical studies of gas adsorption in* $Cu_3(BTC)_2$*: An effective activation procedure*, J. Phys. Chem. C 111 (2007), pp. 9305–9313.

[12] A. Vishnyakov, P.I. Ravikovitch, A.V. Neimark, M. Bu1low, and Q.M. Wang, *Nanopore structure and sorption properties of Cu-BTC metal-organic framework*, Nano Lett. 3 (2003), pp. 713–718.

[13] J. Castillo, T.J.H. Vlugt, and S. Calero, *Understanding water adsorption in Cu-BTC metal-organic frameworks*, J. Phys. Chem. C 112 (2008), pp. 15934–15939.

[14] Q. Yang, C. Xue, C. Zhong, and J. Chen, *Molecular simulation of separation of* CO_2 *from flue gases in Cu-BTC MOF*, AIChE J. 53 (2007), pp. 2832–2840.

[15] Q. Yang and C. Zhong, *Molecular simulation of carbon dioxide/methane/hydrogen mixture adsorption in metal-organic frameworks*, J. Phys. Chem. B 110 (2006), pp. 17776–17783.

[16] S. Wang, Q. Yang, and C. Zhong, *Adsorption and separation of binary mixtures in a metal-organic framework Cu-BTC: A computational study*, Sep. Purif. Technol. 60 (2008), pp. 30–35.

[17] A.I. Skoulidas, *Molecular dynamics simulations of gas diffusion in metal-organic frameworks: Argon in CuBTC*, J. Am. Chem. Soc. 126 (2004), pp. 1356–1357.

[18] A.I. Skoulidas and D.S. Sholl, *Self-diffusion and transport diffusion of light gases in metal-organic framework materials assessed using molecular dynamics simulations*, J. Phys. Chem. B 109 (2005), pp. 15760–15768.

[19] V. Krungleviciute, K. Lask, A.D. Migone, J.-Y. Lee, and J. Li, *Kinetics and equilibrium of gas adsorption on RPM1-Co and Cu-BTC metal-organic frameworks: potential for gas separation applications*, AIChE J. 54 (2008), pp. 918–923.

[20] Materials Studio 3.0 V, Accelrys Inc., San Diego, CA, 2003.

[21] S.J. Goodbody, K. Watanabe, D. MacGowan, J. Walton, and N. Quirke, *Molecular simulation of methane and butane in silicalite*, J. Chem. Soc. Faraday Trans. 87 (1991), pp. 1951–1958.

[22] J.O. Hirschfelder, C.F. Curtiss, and R.B. Bird, *Molecular Theory of Gases and Liquids*, Wiley & Sons, New York, 1954.

[23] J.J. Potoff and J.I. Siepmann, *Vapor–liquid equilibria of mixtures containing alkanes, carbon dioxide, and nitrogen*, AIChE J. 47 (2001), pp. 1676–1682.

[24] F. Darkrim and D. Levesque, *Monte Carlo simulations of hydrogen adsorption in single-walled carbon nanotubes*, J. Chem. Phys. 109 (1998), pp. 4981–4984.

[25] T. Düren, L. Sarkisov, O.M. Yaghi, and R.Q. Snurr, *Design of new materials for methane storage*, Langmuir 20 (2004), pp. 2683–2689.

[26] S. Wang, *Comparative molecular simulation study of methane adsorption in metal-organic frameworks*, Energy & Fuels 21 (2007), pp. 953–956.

[27] G.C. Maitland, M. Rigby, E.B. Smith, and W.A. Wakeham, *Intermolecular Forces: Their Origin and Determination*, Clarendon Press, Oxford, 1981.

[28] G. Maurin, P.L. Llewellyn, and R.G. Bell, *Adsorption mechanism of carbon dioxide in faujasites: Grand canonical Monte Carlo simulations and microcalorimetry measurements*, J. Phys. Chem. B 109 (2005), pp. 16084–16091.

[29] A. Goj, D.S. Sholl, E.D. Akten, and D. Kohen, *Atomistic simulations of CO_2 and N_2 adsorption in silica zeolites: the impact of pore size and shape*, J. Phys. Chem. B 106 (2002), pp. 8367–8375.

[30] G. Garberoglio, A.I. Skoulidas, and J.K. Johnson, *Adsorption of gases in metal organic materials: comparison of simulations and experiments*, J. Phys. Chem. B 109 (2005), pp. 13094–13103.

[31] D. Dubbeldam, H. Frost, K.S. Walton, and R.Q. Snurr, *Molecular simulation of adsorption sites of light gases in the metal-organic framework IRMOF-1*, Fluid Phase Equilib. 261 (2007), pp. 152–161.

[32] H. Tanaka, H. Kanoh, M. Yudasaka, S. Iijima, and K. Kaneko, *Quantum effects on hydrogen isotope adsorption on single-wall carbon nanohorns*, J. Am. Chem. Soc. 127 (2005), pp. 7511–7516.

[33] A.K. Rappé, C.J. Casewit, W.A. Goddard III, and W.M. Skiff, *UFF, a full periodic table force field for molecular mechanics and molecular dynamics simulations*, J. Am. Chem. Soc. 114 (1992), pp. 10024–10035.

[34] V. Krungleviciute, K. Lask, L. Heroux, A.D. Migone, J.-Y. Lee, J. Li, and A. Skoulidas, *Argon adsorption on Cu_3(benzene-1,3,5-tricarboxylate)$_2$(H_2O)$_3$ metal-organic framework*, Langmuir 23 (2007), pp. 3106–3109.

[35] B. Liu, Q. Yang, C. Xue, C. Zhong, and B. Smit, *Molecular simulation of hydrogen diffusion in interpenetrated metal-organic frameworks*, Phys. Chem. Chem. Phys. 10 (2008), pp. 3244–3249.

[36] S. Keskin and D.S. Sholl, *Screening metal-organic framework materials for membrane-based methane/carbon dioxide separations*, J. Phys. Chem. C 111 (2007), pp. 14055–14059.

[37] R. Babarao, Z. Hu, J. Jiang, S. Chempath, and I. Sandler, *Storage and separation of CO_2 and CH_4 in silicalite, C_{168} schwarzite, and IRMOF-1: a comparative study from Monte Carlo simulation*, Langmuir 23 (2007), pp. 659–666.

[38] B. Liu, Q. Yang, C. Xue, C. Zhong, B. Chen, and B. Smit, *Enhanced adsorption selectivity of hydrogen/methane mixtures in metal-organic frameworks with interpenetration: a molecular simulation study*, J. Phys. Chem. C 112 (2008), pp. 9854–9860.

[39] A.R. Millward and O.M. Yaghi, *Metal-organic frameworks with exceptionally high capacity for storage of carbon dioxide at room temperature*, J. Am. Chem. Soc. 127 (2005), pp. 17998–17999.

[40] D. Frenkel and B. Smit, *Understanding Molecular Simulations: From Algorithms to Applications*, 2nd ed., San Diego, CA, Academic Press, 2002.